CDF/PUB/CDFR/PUBLIC/9625
Version 2.0[1]
May 28, 2009

Limits on Gauge-Mediated Supersymmetry-Breaking Models using Diphoton Events with Missing Transverse Energy at CDF II

CDF Collaboration[2]

Abstract

We present the results of an optimized search for a gauge mediated supersymmetry breaking model with $\tilde{\chi}_1^0 \to \gamma\tilde{G}$ with low lifetimes in the $\gamma\gamma$+$\not\!\!E_T$ final state. We observed 0 events using 2.6 fb^{-1} of data collected by CDF II detector, which is consistent with the background estimate of 1.2 ± 0.4 events. We set cross section limits and mass limits as well as interpret our results for lifetimes up to 2 ns and find the exclusion region in the $\tilde{\chi}_1^0$ lifetime vs. mass plane with a mass reach of 149 GeV/c^2 at $\tau(\tilde{\chi}_1^0) = 0$ ns.

1 Introduction

The Standard Model (SM) of elementary particles has been enormously successful, but it is incomplete. For theoretical reasons [1], and because of the '$ee\gamma\gamma$+missing transverse energy ($\not\!\!E_T$)' candidate event recorded by the CDF detector in RUN I [2], there is a compelling rationale to search in high energy collisions for the production of heavy new particles that decay producing the signature of $\gamma\gamma + \not\!\!E_T$.

An example of a theory that would produce such events is gauge mediated supersymmetry breaking (GMSB) [1] with $\tilde{\chi}_1^0 \to \gamma\tilde{G}$ where the $\tilde{\chi}_1^0$ is the lightest neutralino and the next-to-lightest supersymmetric particle (NLSP) and the $\tilde{G}$ is a gravitino which is the lightest supersymmetric particle (LSP). At the Tevatron, above current limits [1], gaugino pair-production is expected to dominate (Figure 1) [1] and the decays produce two $\tilde{\chi}_1^0$'s in association with other particles, with each $\tilde{\chi}_1^0$ decaying into a $\tilde{G}$ (that gives rise to $\not\!\!E_T$) and a photon. Depending on how many of the two $\tilde{\chi}_1^0$'s decay inside the detector, the event has the signature $\gamma\gamma + \not\!\!E_T$, $\gamma + \not\!\!E_T$ or $\not\!\!E_T$ with one or more additional high E_T particles. Previous searches have been performed for low lifetime models in $\gamma\gamma + \not\!\!E_T$ [3, 4] and nanosecond lifetime models in the delayed $\gamma + jet + \not\!\!E_T$ [5, 6] final state.

In this analysis we focus on the $\gamma\gamma + \not\!\!E_T$ final state, as recommended in [7], for low lifetime models of the $\tilde{\chi}_1^0$. The new features of our analysis since the last $\gamma\gamma + \not\!\!E_T$ search with 202 pb^{-1} are to use the EMTiming system [8] to reject non-collision background sources, to use a new *Met Resolution Model* [9] to improve QCD background rejection, and to use 13 times the data (2.6 fb^{-1}).

[1]This result supercedes the results in version 1.0 which was based on 2.0 fb^{-1} data. Differences are listed in an appendix.

[2]Corresponding author: Eunsin Lee

We also extend the search to include our sensitivity to nanosecond $\tilde{\chi}_1^0$ lifetimes which are favored for the large $\tilde{\chi}_1^0$ masses [7].

For concreteness we use the Snowmass Slope constraint (SPS 8) [10] to quote results as a function of $\tilde{\chi}_1^0$ mass and lifetime. While GMSB provides useful limits they are model-dependent, so by keeping our topological cuts to a minumum we keep a quasi model-independent, signature-based approach in our search, as well as providing uesful benchmarks to compare our sensitivity with other searches at DØ [4] and LEP II [6].

Our analysis begins by defining a preselection sample by selecting events with two isolated, central ($|\eta| \lesssim 1.0$) photons with $E_T > 13$ GeV. All candidates are required to pass the standard CDF diphoton triggers, global event selection, standard photon ID, and non-collision background rejection requirements, see Table 1 [3, 9].

The final signal region for this analysis is defined by the subsample of preselection events that also pass a set of optimized final kinematic cuts. The methods for determining the background in the signal region are based on a combination of data and MC and allow for a large variety of potential final sets of cuts. We perform an *a priori* analysis in the sense that we blind the signal region and select the final event requirements based on the signal and background expectations alone. We optimize our predicted sensitivity using a simulation of our GMSB model and calculate, for each GMSB parameter point, the lowest, expected 95% C.L. cross section limit as a function of the following event variables: MetSig, $\Delta\phi(\gamma_1, \gamma_2)$, and H_T, where MetSig is a cut to require the measured $\not\!\!E_T$ in the event to be very significant and H_T is defined as sum of E_T of all EM objects such as photons, electron (isolated, $E_T > 13$ GeV and $|\eta| < 1.2$ if any), any jets (with $E_T > 15$ GeV and $|\eta| < 2.4$) and $\not\!\!E_T$. The MetSig cut gets rid of most of the QCD background with fake $\not\!\!E_T$. In GMSB production heavy gaugino pair-production dominates and the gauginos decay to light, but high E_T, final state particles via cascade decays, which give lots of H_T in the signal compared to the SM backgrounds. The $\Delta\phi(\gamma_1, \gamma_2)$ cut reduces events with back-to-back photons since electroweak backgrounds with large H_T are typically a high E_T photon recoiling againt $W \to e\nu$ where the gauge boson decay is highly boosted.

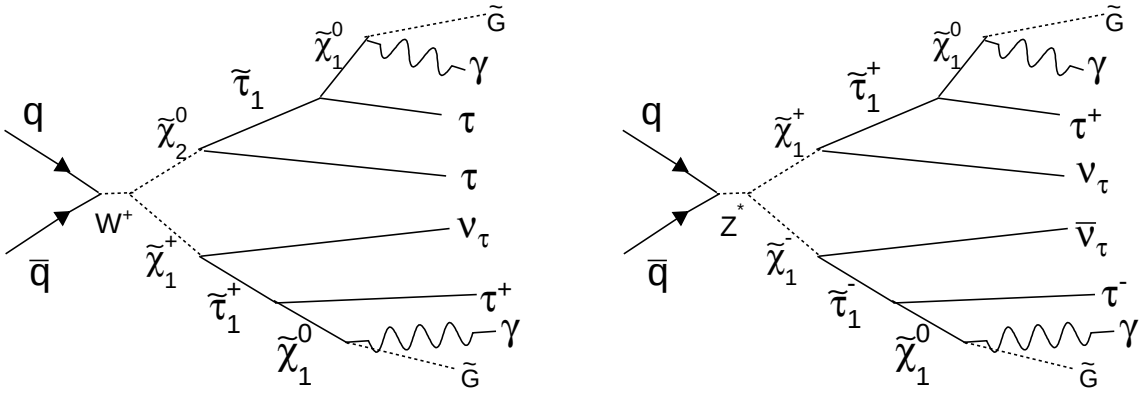

Figure 1: Feynman diagrams of the dominant tree production processes at the Tevatron for the GMSB model line we consider: $\tilde{\chi}_1^{\pm}\tilde{\chi}_2^0$ (45%) (a) and $\tilde{\chi}_1^{\pm}$ pair (b) production (25%). Note that we only show one choice for the charge.

2 Data Selection

The analysis is based on 2.59±0.16 fb^{-1} of data. The analysis selection begins with events that pass the CDF diphoton triggers which is 100% efficient for the final, offline selected γ's. Offline, we require both leading photons to be in the fiducial part of the detector with $|\eta| \leq 1.1$, pass the standard photon ID and isolation requirements and have $E_T^{\gamma} > 13$ GeV. In addition to the standard photon ID cuts we have added additional cuts to suppress PMT spikes [5] and Phoenix rejection cuts [5] to remove events where an electron fakes a prompt photon. Each event is required to have at least one high quality vertex with $|z_{vx}| \leq$60 cm. The E_T of all calorimeter objects (individual towers, photons, electrons, and jets) are calculated with respect to the highest $\sum P_T$ vertex. However, an incorrect vertex can be selected when two or more collisions occur in one beam bunch crossing, making it possible that the highest reconstructed $\sum_{\text{tracks}} p_T$ vertex does not produce the photons. If assigning the photons to a different vertex lowers the $\not\!\!E_T$, we take that $\not\!\!E_T$ and the photon E_T's to be from that vertex for all calculations. We also apply $\not\!\!E_T$ cleanup cuts to remove events where a) if there is evidence that the second photon (γ_2) is partially lost in a crack between detector components and has $|\Delta\phi(\not\!\!E_T, \gamma 2)| < 0.3$, or b) if the event has a jet with $E_T^{\text{jet}} > 5$ GeV, $|\eta| < 2.5$ and $|\Delta\phi(\not\!\!E_T, jet)| < 0.3$. Additional standard topology cuts are placed to reduce non-collision backgrounds, such as cosmic rays and beam halo effects [5]. Our pre-selection sample consists of 38,053 events left after all the quality, ID and cleanup cuts are applied. Table 1 gives a summary of the event reduction.

Requirements	Signal sample (events passed)
Trigger, Goodrun, and Standard photon ID with $\|\eta\| < 1.1$ and $E_T > 13$ GeV	45,275
Phoenix rejection	41,418
PMT spike rejection	41,412
Vertex requirements	41,402
$E_T^{swap} > 13$ GeV after vertex swap	39,719
Beam Halo rejection	39,713
Cosmic rejection (EMTiming cut)	39,663
$\not\!\!E_T$ cleanup cuts	38,053

Table 1: Summary of the $\gamma\gamma$ presample selection requirements and the event sample reduction.

3 Backgrounds

There are three major sources of background for $\gamma\gamma + \not\!\!E_T$ events: QCD events with fake $\not\!\!E_T$, electroweak events with real $\not\!\!E_T$, and non-collision events (PMT spikes, cosmic ray or beam-halo events where one or more of the photons and $\not\!\!E_T$ are not related to the collision).

Standard Model QCD sources, $\gamma\gamma$, $\gamma - jet \rightarrow \gamma\gamma_{fake}$, and $jet - jet \rightarrow \gamma_{fake}\gamma_{fake}$, are the dominant producer of events in the diphoton final state and a major background for $\gamma\gamma$ with fake $\not\!\!E_T$. These backgrounds come in two different categories; fake $\not\!\!E_T$ due to energy measurement fluctuations in the calorimeter as measured by our *Met Model*, and fake $\not\!\!E_T$ due to pathologies such as picking the wrong vertex in events where true collision did not create a vertex or tri-photon events with a lost photon. The energy measurement fluctuations in the calorimeter, which lead to considerable values of fake $\not\!\!E_T$, happen only in a small fraction of cases, but huge cross sections

for these processes make them one of the largest backgrounds. However, rather than measure $\not\!\!E_T$, we can significantly reduce the QCD background by selecting events based on MetSig, using a new *Met Resolution Model* [9].

The *Met Resolution Model* considers the clustered and unclustered energy in the event and calculates a probability, $P(\not\!\!E_T{}^{fluct} > \not\!\!E_T)$, for fluctuations in the energy measurement to produce $\not\!\!E_T{}^{fluct}$ equivalent to or larger than the measured $\not\!\!E_T$. This probability is then used to define MetSig $= -\log_{10}\left(P_{\not\!\!E_T{}^{fluct} > \not\!\!E_T}\right)$. Events with true and fake $\not\!\!E_T$ of the same value should have, on average, different MetSig. For each data event we throw 10 pseudo-experiments to generate a $\not\!\!E_T$ and calculate its significance, according to the jets and underlying event configuration. Then we count the number of events in the pseudo-experiments that pass our MetSig and other kinematic cuts. This number, divided by the number of pseudo-experiments, gives us the *Met Model* prediction. The systematic uncertainty on the number of events above a MetSig cut is evaluated by comparing the *Met Model* predictions with the default set of model parameters to predictions obtained with the parameters deviated by $\pm\sigma$. The total uncertainty is estimated by adding the statistical uncertainty on the number of pseudo-experiments passing the cuts and these systematic uncertainties in quadrature.

A source of QCD background that is unaccounted for by the *Met Model* is diphoton candidate events with event reconstruction pathologies such as a wrong choice of the primary interaction vertex and tri-photon events with a lost photon. To obtain the prediction for all events reconstruction pathologies in the QCD background at the same time, we model the kinematics and event reconstruction using a PYTHIA [11] $\gamma\gamma$ sample, with large statistics, and normalize to the number of events in the presample to take into account jet backgrounds. Then we subtract off the expectations for energy mismeasurement fluctuations in the MC to avoid double counting. The systematic uncertainties on this background prediction include the uncertainty on the scale factor and the uncertainty due to MC-data differences in the unclustered energy parameterization and the jet energy scale.

Electroweak processes involving W's and Z's are the most common source of real and significant $\not\!\!E_T$ in $p\bar{p}$ collisions. We estimate the background rate from decays into both charged and neutral leptons. There are four ways we can get a $\gamma\gamma + \not\!\!E_T$ signature in electroweak events that decay into one or more charged leptons: 1) from $W\gamma\gamma$ and $Z\gamma\gamma$ events where both photons are real; 2) from $W\gamma$ and $Z\gamma$ events with a fake photon; 3) from W and Z events where both photon candidates are fake photons; and 4) $t\bar{t}$ production and decay. To estimate the contribution from the electroweak backgrounds we use the Baur and PYTHIA MC's [11], according to their production cross section and k-factors, but normalized to data. The Baur MC simulation of $W\gamma$ and $Z\gamma$ are used to evaluate contributions from both $W/Z + \gamma$ and $W/Z + \gamma\gamma$ events using ISR/FSR. Inclusive W and Z samples produced from PYTHIA are used to obtain the contribution from $W + jet$ and $Z + jet$ events where both photon candidates are fakes and $t\bar{t}$ events. We consider all three charged leptonic decay modes of W and Z bosons. The electroweak background predictions are given by

$$\mathrm{N}^{\mathrm{EWK}}_{\mathrm{signal}} = \sum_{i=0}^{n} \mathrm{N}^{\mathrm{EWK-MC}}_{\mathrm{signal},i} \cdot \mathrm{SF}_i \cdot \left(\frac{\mathrm{N}^{\mathrm{Data}}_{e\gamma,\mathrm{signal}}}{\mathrm{N}^{\mathrm{MC}}_{e\gamma,\mathrm{signal}}} \right) \tag{1}$$

where $\mathrm{N}^{\mathrm{EWK-MC}}_{\mathrm{signal},i}$ is the number of events passing all the final kinematic cuts from MC sample i, for each electroweak source. The scale factors, SF_i, normalizes each electroweak background to its production cross section and k-factor. To minimize the dependence of our predictions on potential Data-MC differences (trigger efficiencies, acceptance and ID efficiencies, modeling of ISR/FSR, PDF uncertainties, luminosity uncertainties, etc.), we normalize, using the rate of the number of $e\gamma$ events observed in the data that also pass all signal kinematic cuts, to the number of events

observed in MC. This $e\gamma$ sample is derived from diphoton trigger datasets and the events are required to pass the preselection requirements where electrons are required to pass photon-like ID requirements [9]. The uncertainty on the electroweak backgrounds are dominated by the $e\gamma$ normalization factor uncertainty. This includes data and MC statistical uncertainties as well as differences in MC modeling. The total uncertainties also include the MC statistical uncertianties and uncertainties on the normalization factors added in quadrature.

To estimate the electroweak backgrounds from neutral leptonic channels such as $Z\gamma\gamma \to \nu\bar{\nu}\gamma\gamma$, $Z\gamma \to \nu\bar{\nu}\gamma + \gamma_{fake}$ or $Z \to \nu\bar{\nu} + \gamma_{fake}\gamma_{fake}$, we use a MadGraph $Z(\mu^+\mu^-) + \gamma\gamma$ sample[3]. Using this sample we remove photons from lepton FSR to estimate $Z\gamma\gamma \to \nu\bar{\nu}\gamma\gamma$ since neutrinos do not radiate photons. Similarly we exactly consider events with $86 < \mathrm{M}_Z^{\mathrm{HEPG}} < 96$ GeV since there is no Z/γ^* interaction in $\nu\bar{\nu}$ final states. The number of events in the signal region is then estimated to be the number of events that pass all the final kinematic cuts, normalized to the production cross section, luminosity, k-factor and including the electroweak scale factors.

Non-collision backgrounds to the $\gamma\gamma + \not\!\!E_T$ background come from beam halo (B.H.) and cosmic rays (C.R.) where either a single or double photon-like signature comes from the non-collision source. Because these events do not originate from beam-beam interactions, they can be a source of significant spurious $\not\!\!E_T$.

The dominant source of beam halo events that fake the $\gamma\gamma + \not\!\!E_T$ final state occur when high energy muons, produced in beam-beam pipe interactions, interact with the calorimeter and fake two photons [5]. To estimate the rate at which the B.H. events contribute to the $\gamma\gamma + \not\!\!E_T$ final state, we use a beam halo enriched $\gamma\gamma$ sample selected as having two loose photon candidates, but also identified as being due to a beam halo. To increase the statistics we do not require a vertex, nor do we reject events that fail the EMTiming requirements. To take this sample to the prediction of the number of events in the signal region we multiply by the measured rate at which these events pass the kinematic cuts as well as the rate they pass the ID and isolation, vertex and timing cuts. Finally we take into account the efficiency for B.H. events to be in this sample. The uncertainties on background rate in the signal region are dominated by the statistical uncertainty on the number of events after all kinematic cuts in the B.H. control sample. The other source of uncertainty, though much smaller, is the uncertainty on fraction of B.H. events that pass the vertex, ID and EMTiming cuts.

The dominant source of cosmic ray muon events that fake the $\gamma\gamma + \not\!\!E_T$ signature come via photon Bremsstrahlung as the muon traverses the magnet, or by catastrophic interaction with the EM calorimeter. We select a cosmic ray enriched sample of two photons passing the loose photon ID cuts, but failing the timing cuts. Specifically, at least one of the photon candidate must have $\mathrm{T}_\gamma > 25$ ns. That way we take into account all cosmic ray sources; both photons from the same cosmic ray, both photons from different cosmic rays, and one photon from a cosmic ray and one from the collision. To increase the sample statistics, events are not required to pass our vertex cut ($|Z_{vx}| < 60$ cm), which we correct for in our sample estimate, using similar techniques as above. The uncertainties are dominated by statistical uncertaintiy on the number of identified cosmics events.

After estimating the MetSig distributions for all the backgrounds, where the QCD is normalized to the data, the expected MetSig distribution for the presample is shown in Figure 2. With these tools in hand we are set to estimate the backgrounds for a large variety of cuts and move to an estimation of the acceptance for GMSB models in the signal region for use in optimization.

[3] A $Z \to \nu\bar{\nu}$ sample with high statistics is in progress.

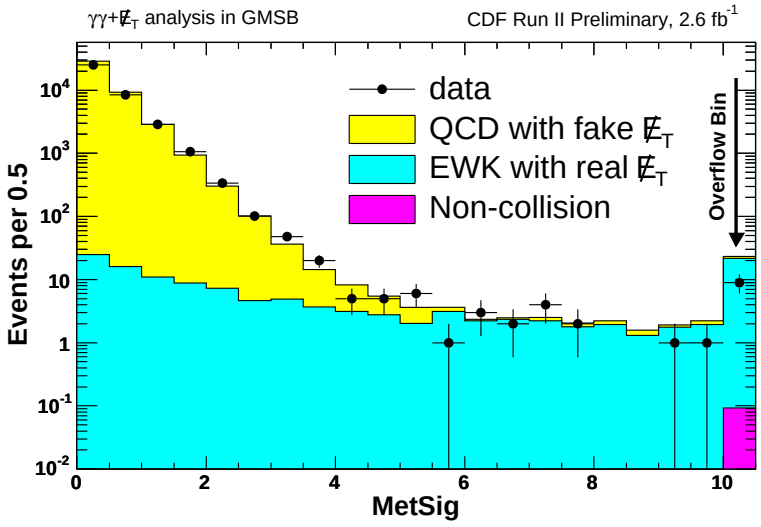

Figure 2: The background predictions for the presample. The highest MetSig bin includes all overflow events.

4 GMSB Signal Monte Carlo and Systematic Uncertainties

To estimate the acceptance for GMSB we use the PYTHIA event generator [11] as well as a full detector simulation [12]. For the purpose of this analysis we consider a GMSB model with parameters fixed on the minimal-GMSB Snowmass slope constraint (SPS 8) that is commonly used [3, 6]. All SUSY production processes are simulated [11]. The breakdown of events after passing each of the selection cuts for an example GMSB point at $m(\tilde{\chi}_1^0) = 140$ GeV and $\tau(\tilde{\chi}_1^0) = 0$ ns near the limit, is shown in Table 2. For completeness we have included the results for the final event selection, determined in Section 5.

Requirement	Events passed	$A_{\text{Signal MC}}$ (%) ($m(\tilde{\chi}_1^0) = 140$ GeV and $\tau(\tilde{\chi}_1^0) = 0$ ns)
Sample events	133330	100.0
Two EM Objects and $\lvert z_{vertex}\rvert < 60\ cm$	124771	93.6
Photon fiducial and Standard ID cuts ($\lvert\eta\rvert < 1.1$ and $E_T > 13$ GeV)	18270	13.7
Phoenix Rejection & PMT cuts	17625	13.2
Beam Halo and Cosmic Rejection cuts	17612	13.2
Vertex Swap and $\not\!\!E_T$ Cleanup cuts	17049	12.8
MetSigi>3	12610	9.5
H_T>200 GeV	11913	8.9
$\Delta\phi(\gamma_1, \gamma_2)<\pi - 0.35$	10395	7.8

Table 2: Summary of the event reduction for a GMSB example point in the $\gamma\gamma$+$\not\!\!E_T$ final state. We have included the final, optimized cuts for completeness.

Since we estimate the sensitivity of the search to be equal to the expected 95% C.L. cross section limits, we need the uncertainties for the trigger, luminosity, background and acceptance. As mentioned in Section 2, with our combination of triggers we take a trigger efficiency of 100% with negligible error. The systematic uncertainty on the luminosity is taken to be 6% with major contributions from the uncertainties on the CLC acceptance from the precision of the detector

simulation and the event generator [11]. The systematic uncertainty on the background in the signal region is determined from our understanding of both the collision and non-collision sources, as described in Section 3. The background uncertainty is evaluated for every set of cuts in the optimization procedure. The systematic uncertainty on the signal acceptance for an example GMSB point of $m(\tilde{\chi}_1^0) = 140$ GeV and $\tau(\tilde{\chi}_1^0) = 0$ ns is estimated to be 6.9% with major contributions from diphoton ID and isolation efficiency (5.4%) and ISR/FSR (3.9%). The uncertainty on the NLO production cross section is dominated by the uncertainty from PDFs (7.6%) and the renormalization scale (2.6%) for a total of 8.0%. All uncertainties are included in the final cross section limit calculation, and we take the acceptance and production cross section uncertainties in quadrature for a total uncertainty of 10.6%.

5 Optimization and Results

Now that the background is estimated and the signal acceptance is available for a variety of cuts, an optimization procedure can be readily employed to find the optimal cuts before unblinding the signal region. We optimize for the following cuts: MetSig, H_T, and $\Delta\phi(\gamma_1, \gamma_2)$.

As described in Section 3, the MetSig cut gets rid of most of the QCD background with fake $\not\!\!E_T$. The H_T cut separates between the high E_T, light final state particles produced by GMSB events via cascade decays and SM backgrounds, dominated by QCD and electroweak backgrounds, which do not have lots of high E_T objects. The $\Delta\phi(\gamma_1, \gamma_2)$ cut gets rid of events where two photons are back to back since electroweak backgrounds with large H_T are typically a high E_T photon recoiling against $W \to e\nu$, which means the gauge boson decay is highly boosted. Also the high E_T diphoton with large H_T from QCD background are mostly back-to-back with fake $\not\!\!E_T$ or wrong vertex.

By estimating our sensitivity using the 95% C.L. expected cross section limits on GMSB models in the no-signal assumption, we find the optimal set of cuts before unblinding the signal region. We use the standard CDF cross section limit calculator [13] to calculate the limits, taking into account the predicted number of background events, the acceptance, the luminosity and their systematic uncertainties.

For each GMSB point there is a minimum expected cross section limit as a function of the kinematic cuts. Figures 3-(a), (c), and (e) show the expected cross section limit as a function of a cut after keeping all other cuts fixed at the already optimized values, showing it is at the minimum. We decided to use a single set of cuts before we open the box based on the expectation that they will yield the largest expected exclusion region. We chose: MetSig>3, H_T>200 GeV, $\Delta\phi(\gamma_1, \gamma_2)<\pi - 0.35$ rad. With these cuts we predict a total of 1.23±0.38 background events. The dominant electroweak contributions are $Z\gamma \to \mu\mu\gamma$ and $Z\gamma \to \nu\nu\gamma$ which produce a total of 0.19±0.10 and 0.11±0.03 events respectively. The QCD background is dominated by energy measurement fluctuations in the $\not\!\!E_T$, estimated using the *Met Model*, to have a rate of 0.40±0.20 events. The non-collision backgrounds are dominated by cosmics which have a rate of 0.001±0.001 events. Table 3 provides a summary. Figures 3-(b), (d), and (f) show the distributions of each optimization variable normalized to the number of expected events, after applying all optimized cuts. We compare the background distribution before unblinding the signal region and the expected signal in the signal region for an example GMSB point at $m(\tilde{\chi}_1^0) = 140$ GeV and $\tau(\tilde{\chi}_1^0) = 0$ ns. Taking into account the errors we expect an acceptance of (7.8±0.5)% and 4.6±0.6 events for this point.

After all optimal cuts we open the box and observe no events, consistent with the expectation of 1.2±0.4 events. We show the kinematic distributions for the background and signal expectations

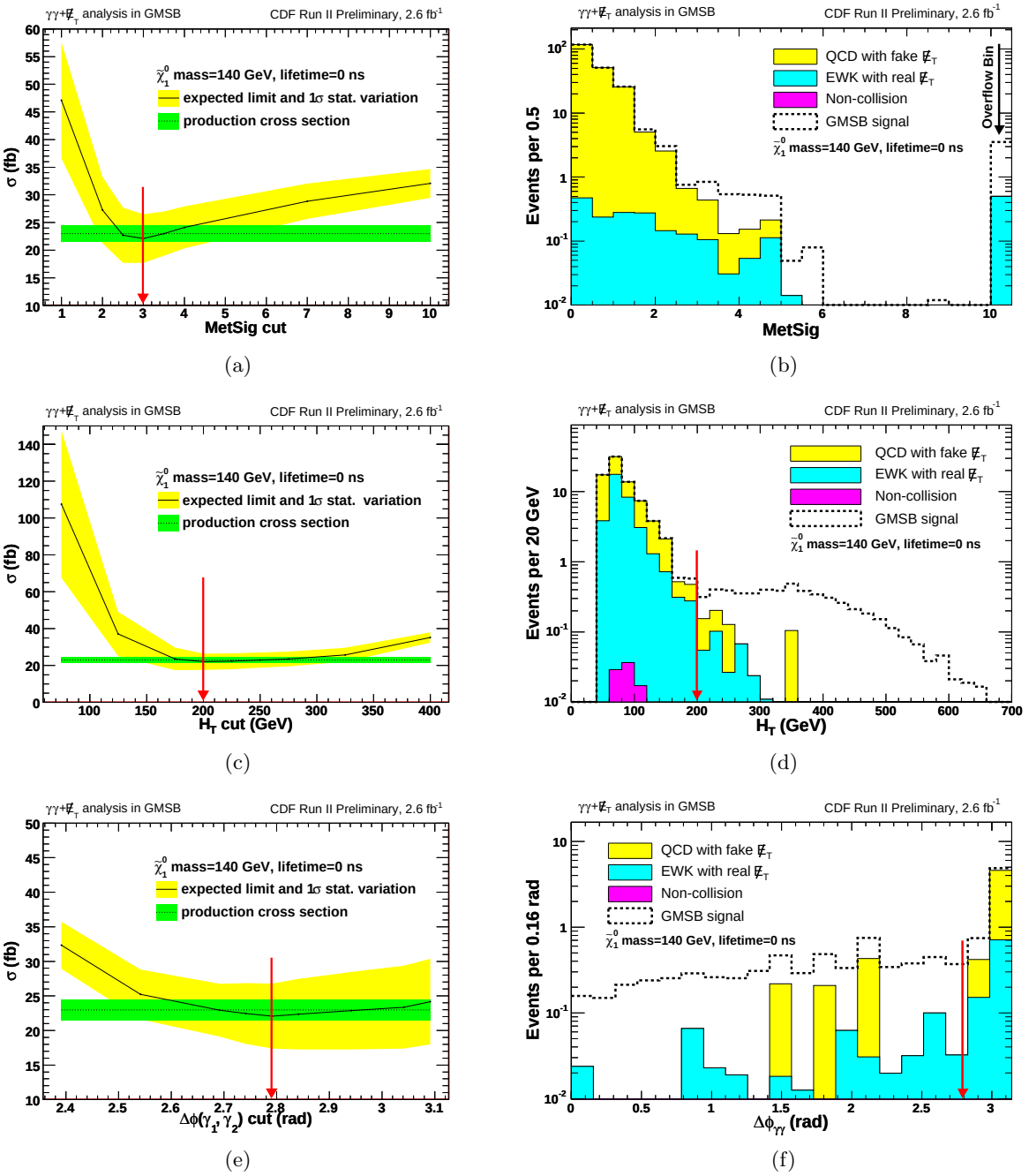

Figure 3: The expected 95% C.L. cross section limit as a function of the MetSig (a), H_T (c), and $\Delta\phi(\gamma_1,\gamma_2)$ (e) requirements for a GMSB example point ($m(\tilde{\chi}_1^0) = 140$ GeV and $\tau(\tilde{\chi}_1^0) = 0$ ns). All other cuts held at their optimized values. The optimal cut is where the expected cross section is minimized. Indicated in green is the 8.0% uncertainty-band for the production cross section and in yellow is the RMS. The N-1 predicted kinematic distributions after the optimized requirements are shown in Figure (b), (d), and (f). Note that in (b) bins at MetSig=10 are overflows.

Background Source	Expected Rate±Stat±Sys
Electroweak	0.77±0.21±0.22
QCD	0.46±0.22±0.10
Non-Collision	$0.001^{+0.008}_{-0.001} \pm 0.001$
Total	1.23±0.30±0.24

Table 3: Summary of the combined background estimations after optimization. Note we have ignored the small asymetric uncertainty in the total calculation.

along with the data in Figure 4. There is no distribution that hints at an excess and the data appears to be well modeled by the background prediction alone.

We show the predicted and observed cross section limits along with the NLO production cross section, which is calcuated by multiplying the PYTHIA LO cross section calculation by k-factor [14], as a function of $\tilde{\chi}_1^0$ mass at a lifetime of 0 ns and as a function of lifetime at a mass of 140 GeV/c^2 in Figure 5. Since the number of observed events is below expectations the observed limits are slightly better than the expected limits. The $\tilde{\chi}_1^0$ mass reach, based on the predicted (observed) number of events is 141 GeV/c^2 (149 GeV/c^2), at a lifetime of 0 and 1 ns. We do not consider lifetimes above 2 ns as the expectation that most of the parameter space in high lifetimes there should be covered by searches in single delayed photon analysis [5, 7]. We show the 95% C.L. NLO exclusion region as a function of mass and lifetime of $\tilde{\chi}_1^0$ using the fixed choice of cuts from the optimization for both for the predicted and observed number of background events in Figure 6. These limits extend the reach beyond the CDF delayed photon results [5] and well beyond those of DØ searches at $\tau = 0$ [4] and the limit from ALEPH/LEP [6], and are currently the world's best.

6 Conclusions and Prospects for the future

We have set limits on GMSB models using the $\gamma\gamma + \not\!\!E_T$ final state. Candidate events were selected based on 13 times more data, the new $\not\!\!E_T$ resolution model technique, the EMTiming system and a full optimization procedure. We found 0 events using 2.6 fb^{-1} of data in run II which is consistent with the background estimate of 1.2±0.4 events from the Standard Model expectations. We showed exclusion regions and set limits on GMSB models with a $\tilde{\chi}_1^0$ mass reach of 149 GeV/c^2 at a $\tilde{\chi}_1^0$ lifetime of 0 ns. Our results extend the world sensitivity to these models.

To investigate the prospects of a search at higher luminosity we calculate the cross section limits assuming all backgrounds scale linearly with luminosity while their uncertainty fractions remain constant. Figure 7 shows the predicted exclusion region for a luminosity of 10 fb^{-1}. For higher lifetimes (above ∼2 ns) the next generation delayed photon analysis will extend the sensitiviy taken from Ref. [5] and then will combine these results for completeness.

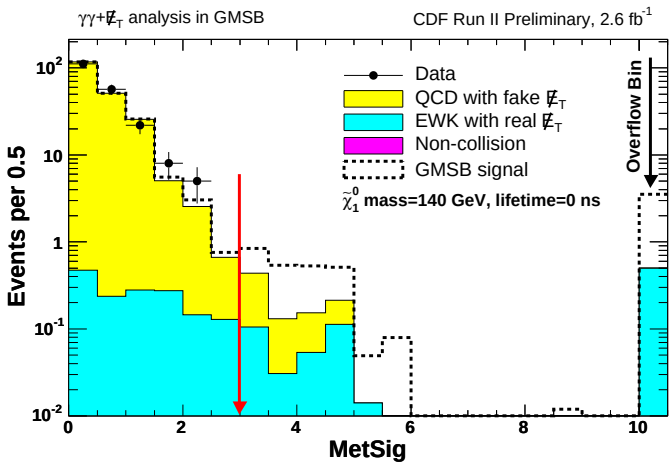

(a)

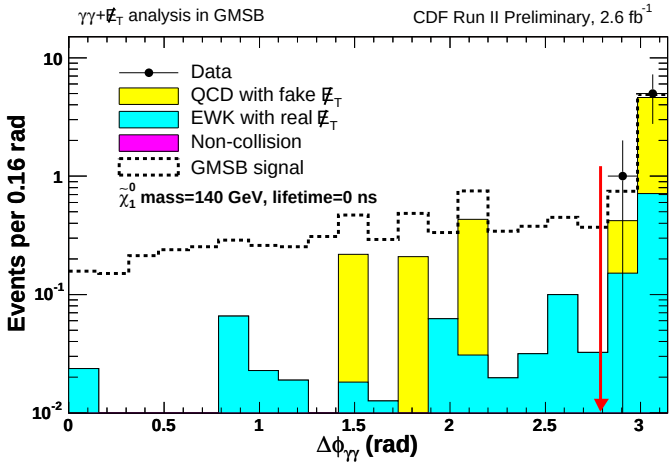

(b)

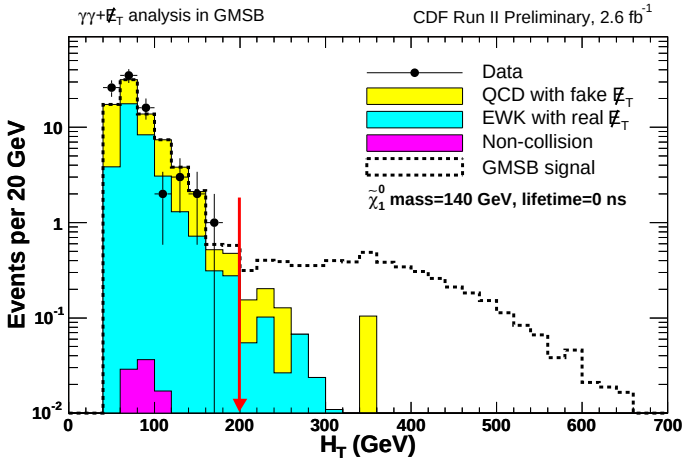

(c)

Figure 4: The same N-1 plots as Figure 3, but including the data. Each variable is plotted through the whole region while holding other variables at the optimal cuts. There is no evidence for new physics and the data is well modeled by backgrounds alone. The highest bin in (a) includes all overflow events.

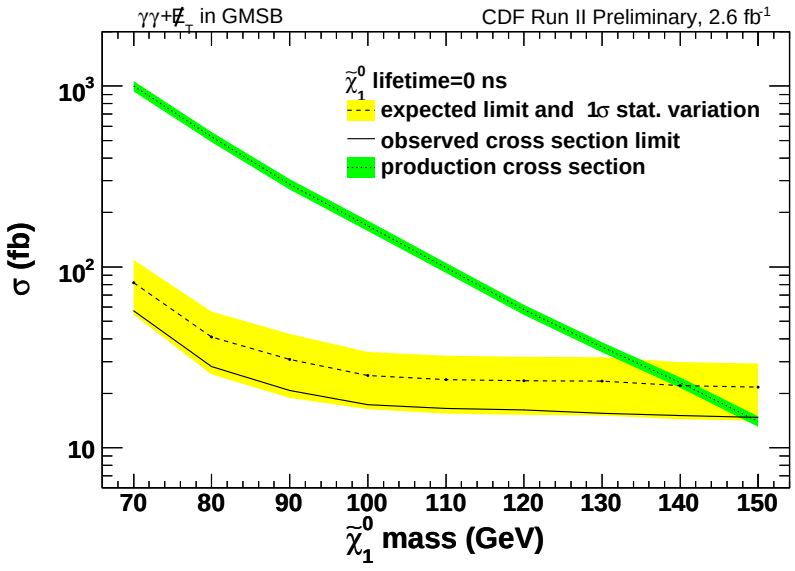

(a)

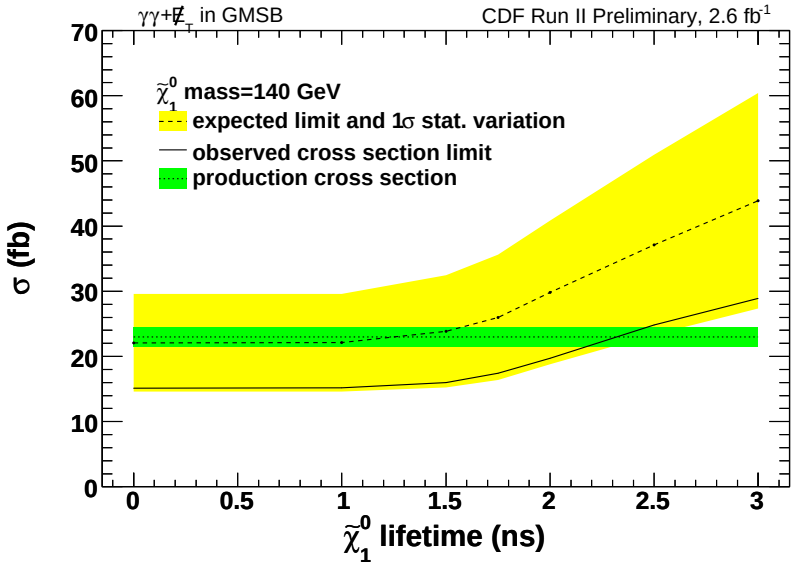

(b)

Figure 5: The predicted and observed cross section limits as a function of the $\tilde{\chi}_1^0$ mass at a lifetime of 0 ns (a) and as a function of the $\tilde{\chi}_1^0$ lifetime at a mass of 140 GeV/c^2 (b). Indicated in green is the 8.0% uncertainty-band for the production cross section, in yellow the RMS variation in the expected on the cross section limit.

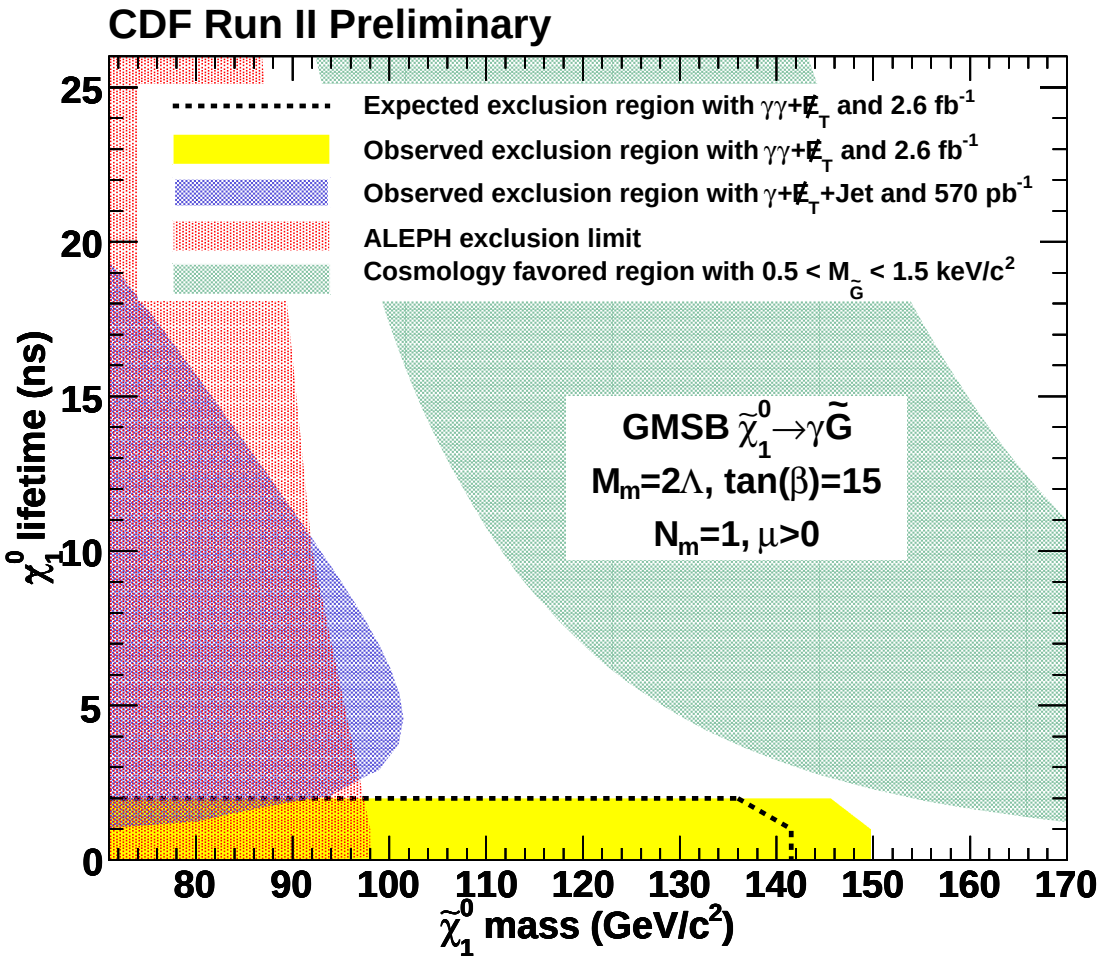

Figure 6: The predicted and observed exclusion region along with the limit from ALEPH/LEP [6] and the $\gamma + \not\!\!E_T + jet$ delayed photon analysis [5]. We have a mass reach of 141 GeV/c^2 (predicted) and 149 GeV/c^2 (observed) at the lifetime up to 1 ns. The green shaded band shows the parameter space where $0.5 < m_{\tilde{G}} < 1.5$ keV/c^2, favored in cosmologically consistent models [15].

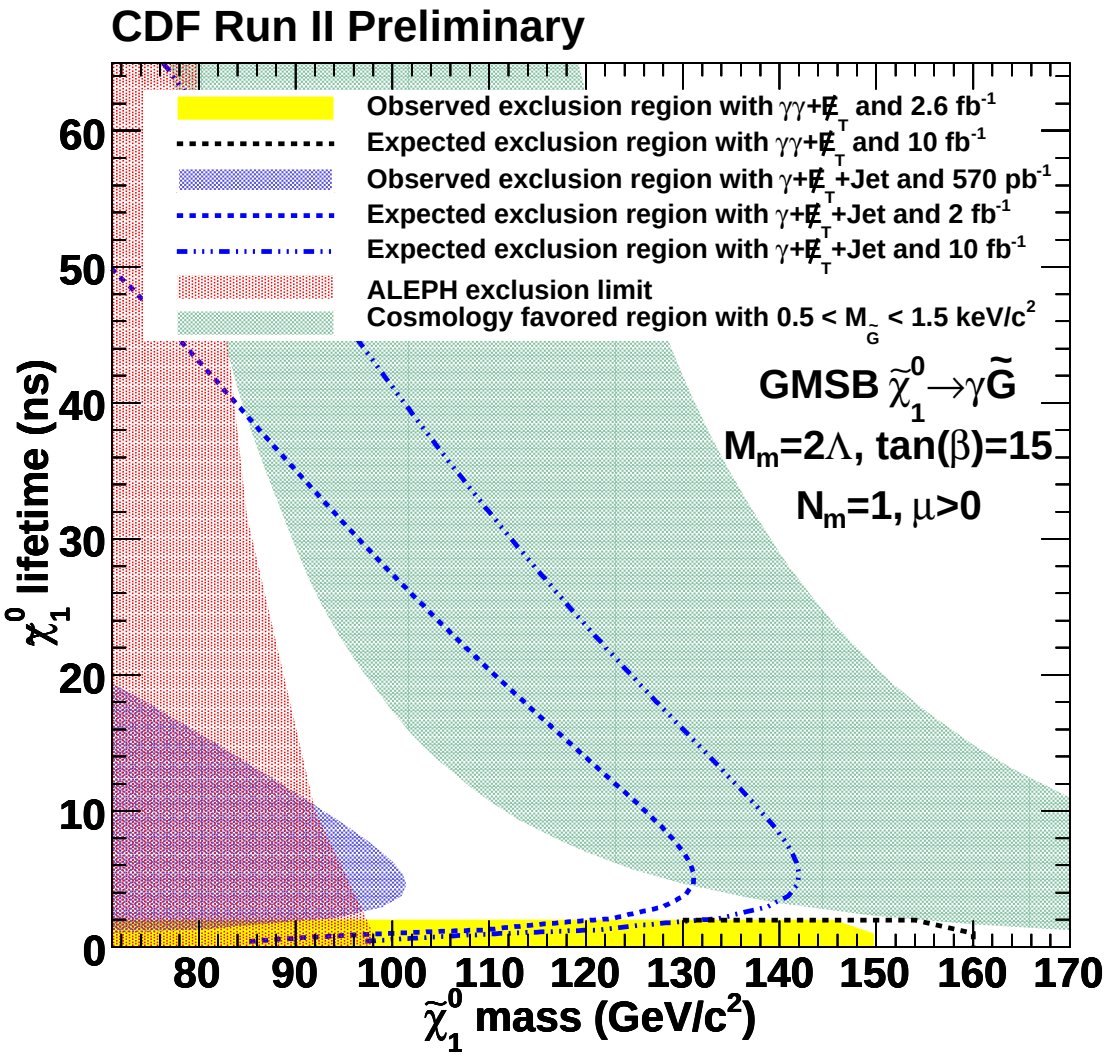

Figure 7: The projected sensitivity to GMSB models with more data. The black dashed line shows the prediction of the exclusion region limit after a scaling of the background prediction and the uncertainties for a luminosity of 10 fb^{-1}. The blue dashed lines show the prediction of the exclusion region limits from the delayed photon analysis for a luminosity of 2 fb^{-1} and 10 fb^{-1} respectively taken from Ref. [5].

A Appendix-I: Changes Since the 2 fb^{-1} Analysis

The results of the search for GMSB models in the $\gamma\gamma + \not\!\!E_T$ final state with 2 fb^{-1} of data were blessed on November 6, 2008 as described in version 1.0 of this note. In this section, we present a brief summary of changes and improvements compared to the previous measurement.

- Added 1.0 fb^{-1}, which has high instantaneous luminosity, and dropped 0.4 fb^{-1}, which has low instantaneous luminosity and no EMTiming information. Now all data has the EMTiming information. This allows for a single set of simple and efficient ways to remove cosmic rays and beam halo events. We dropped the old inefficient, cosmic cuts.
- We switched to using a vertex swap procedure to remove wrong vertex events and added $\not\!\!E_T$ cleanup cuts to get rid of tri-photon events with a lost photon.
- We realized that the backgrounds reported had the $\not\!\!E_T$ cleanup and wrong vertex cuts on them. Since we now use them explicitly, this requires no changes.
- We added $Z \to \nu\nu$ to electroweak backgrounds.
- We did a more complete estimate of the systematic uncertainties. In the previous anaysis we used 18%, taken from 202 pb^{-1} analysis [3], to be conservative. Now it is reduced to 10.6% since the uncertainty on photon ID and isolation efficiencies is smaller due to improved understanding of the detector.
- We re-optimize after these changes and found that only the $\Delta\phi(\gamma_1, \gamma_2)$ cut needed to change from π-0.15 (2.99) to π-0.35 (2.79).
- We found that the formulae used to produce the cosmology favored region band in Figures 6 and 7 is incorrect. We now produce the band correctly according to Ref [1].

References

[1] See for example S. Ambrosanio, G. L. Kane, G. D. Kribs, S. P. Martin and S. Mrenna, Phys. Rev. D **54**, 5395 (1996) or C. H. Chen and J. F. Gunion, Phys. Rev. D **58**, 075005 (1998).

[2] CDF Collaboration, F. Abe *et al.*, Phys. Rev. Lett. **81**, 1791 (1998); Phys. Rev. D **59**, 092002 (1999).

[3] CDF Collaboration, D. Acosta *et. al.*, Phys. Rev. D **71**, 031104 (2005).

[4] DØ Collaboration, V.M. Abazov *et. al.*, Phys. Lett. B **659**, 856 (2008).

[5] CDF Collaboration, A. Abdulencia *et. al.*, Phys. Rev. Lett **99**, 121801 (2007); CDF Collaboration, T.Aaltonen *et. al.*, Phys. Rev. D **78**, 032015 (2008).

[6] ALEPH Collaboration, A. Heister *et. al.*, Eur. Phys. J. C **25**, 339 (2002); A. Garcia-Bellido, Ph.D. thesis, Royal Holloway University of London (2002) (unpublished), arXiv:hep-ex/0212024.

[7] P. Wagner and D. Toback, Phys. Rev. D **70**, 114032 (2004).

[8] M. Goncharov *et. al.*, NIM A**565**, 543 (2006).

[9] R. Culbertson, A. Pronko, S. Yu, M. Goncharov, CDF public note 9339.

[10] B. C. Allanach *et. al.*, Eur. Phys. J. C**25**, 113 (2002).

[11] PYTHIA: T. Sjöstrand, L. Lönnblad and S. Mrenna, JHEP **0612** 046 (2005); *cdfsoft* 6.1.4 has PYTHIA version 6.216; Baur: U. Baur, T Han and J. Ohnemus, Phys. Rev. D **57**, 2823 (1998)

[12] *cdfSim*: G.S. Sganos, Tutorial on cdfSim. We modified it for the simulation of the EMTiming system [7].

[13] E. Boos, A. Vologdin, D. Toback and J. Gaspard, Phys. Rev. D **66**, 013011 (2002). J. Conway, CERN Yellow Book Report No. CERN 2000-005 (2000), p. 247.

[14] W. Beenakker, *et al.*, Phys. Rev. Lett. **83**, 3780 (1999).

[15] J. L. Feng and T. Moroi, Phys. Rev. D **70**, 075019 (2004).